Electronic supplementary information

A novel all-solid-state asymmetric supercapacitor with superior electrochemical performance in a wide temperature range by using hydroquinone modified graphene xerogel as cathode and N-doped $Ti_3C_2T_x$ as anode

Qimeng Sun,[a] Tao He[b] and Yueming Li[*a]*

a. State Key Laboratory of Metastable Materials Science and Technology, College of Materials Science and Engineering, Yanshan University, Qinhuangdao 066004, China
b. Shanghai Advanced Research Institute, Chinese Academy of Sciences, Shanghai, China

[*] Corresponding author: Prof. Yueming Li, Tel: 86-335-807-4631, E-mail: liyueming@ysu.edu.cn

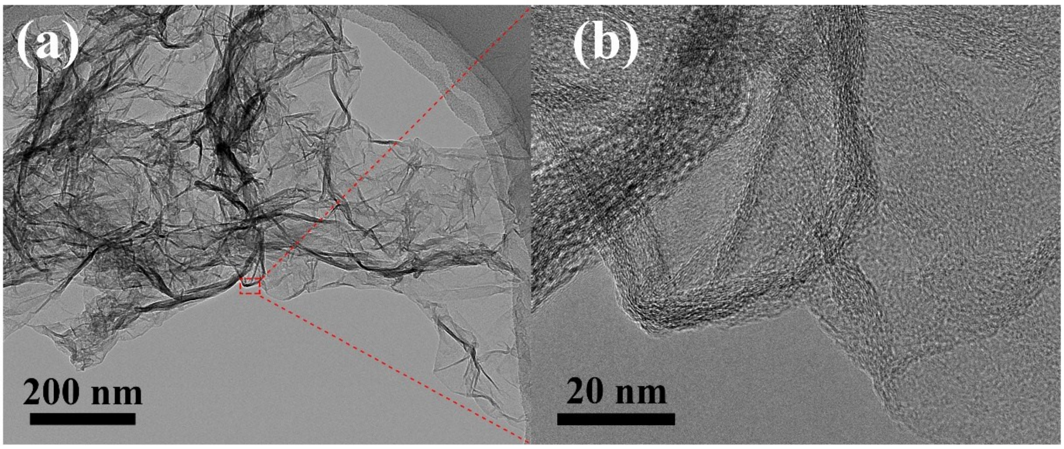

Figure S1 (a) TEM image and (b) HRTEM image of the HG2.

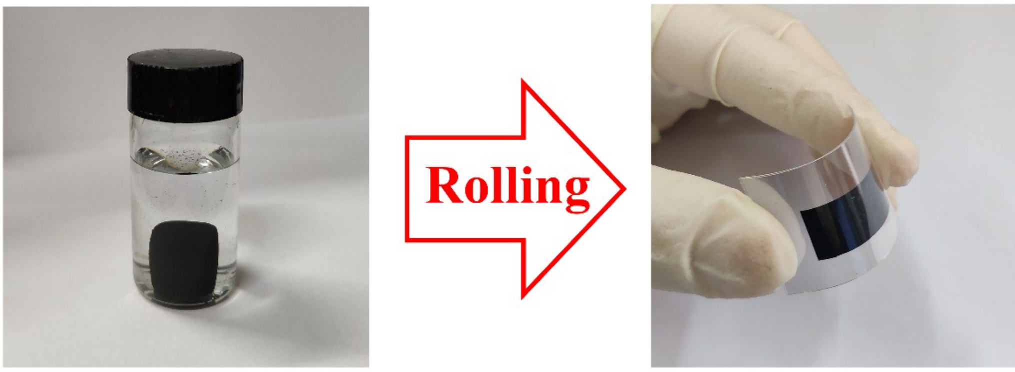

Figure S2: Prepared graphene hydrogel and graphene electrode prepared by rolling.

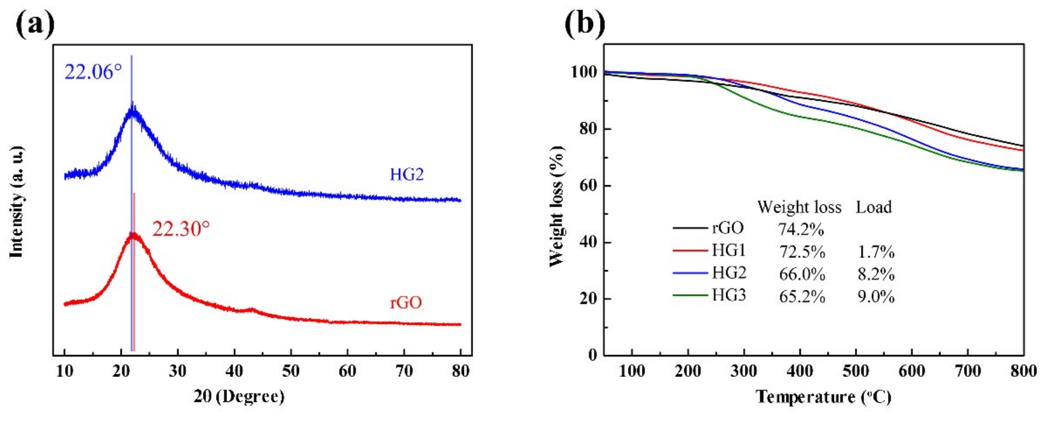

Figure S3 (a) XRD patterns of rGO and HG2. (b) TGA curves of rGO and HG2 samples in Ar at a heating rate of 5 °C min^{-1}.

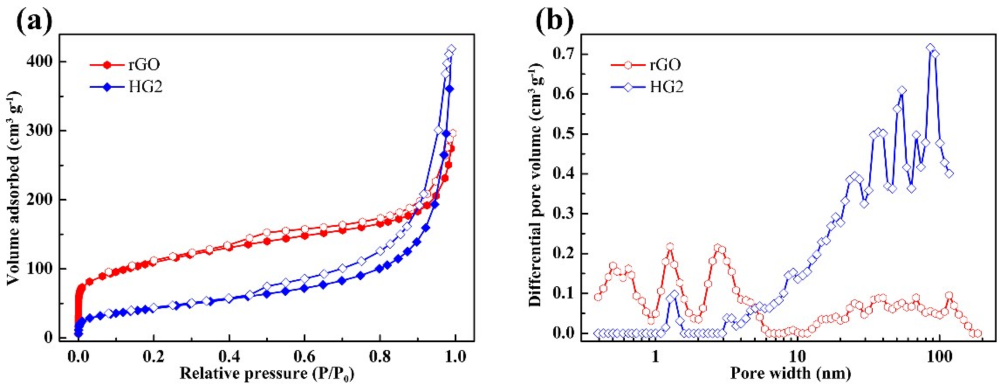

Figure S4 Nitrogen adsorption-desorption isotherm (a), and pore width distribution (b) for rGO and HG2.

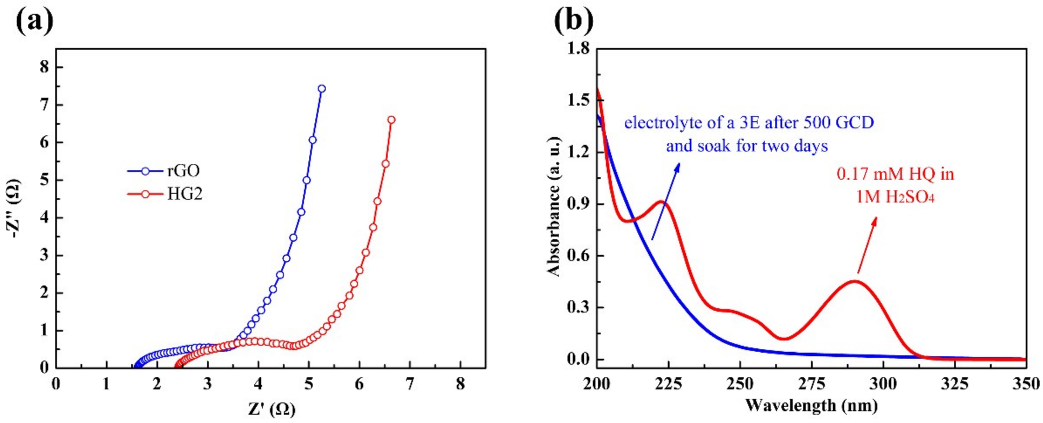

Figure S5: (a) Nyquist plots of rGO and HG2 electrodes at room temperature. (b) UV-vis absorption spectra of a 0.17 mM HQ in 1 M H_2SO_4 solution and the electrolyte which was after 500s CD at low current density of 2 A g^{-1} and soak for two days in the three-electrode device.

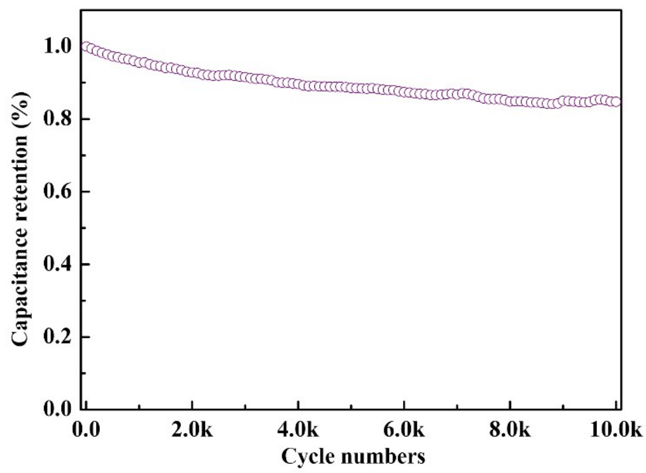

Figure S6 Cycling stability at 20 A g^{-1} of the HG2 electrode at room temperature.

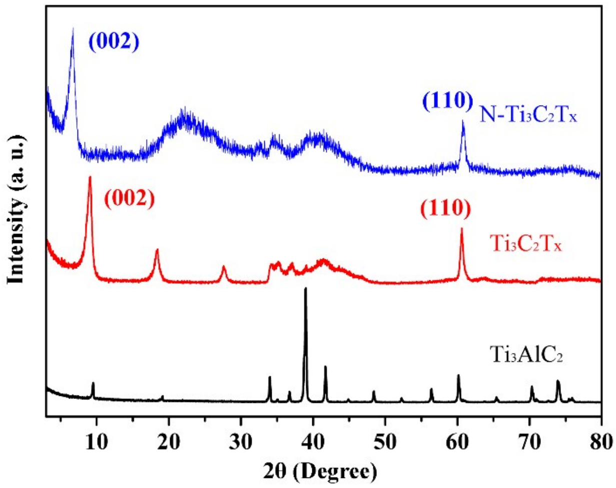

Figure S7 XRD patterns of Ti_3AlC_2, $Ti_3C_2T_x$ and N-$Ti_3C_2T_x$.

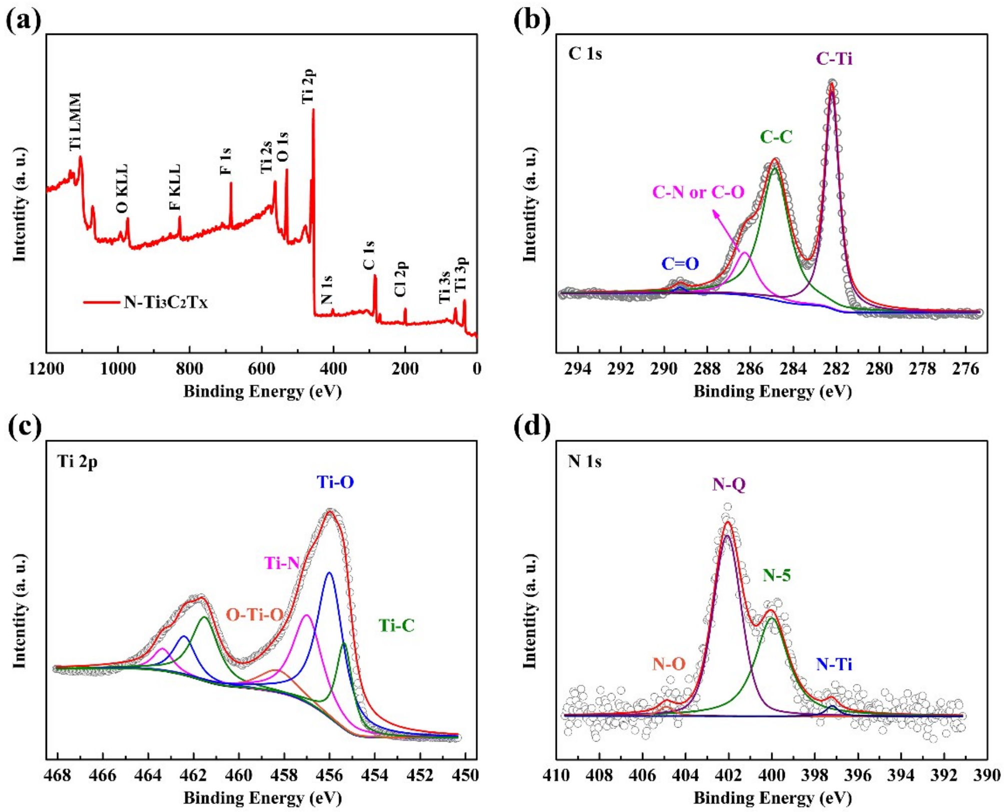

Figure S8 (a) XPS spectrum for N-$Ti_3C_2T_x$. (B) High-resolution XPS spectra of C 1s (b), Ti 2p (c) and N 1s (d) for N-$Ti_3C_2T_x$.

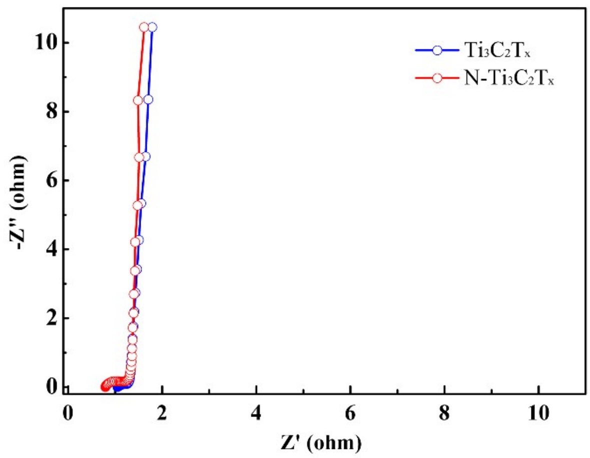

Figure S9 Nyquist plots of $Ti_3C_2T_x$ and $N-Ti_3C_2T_x$ at room temperature.

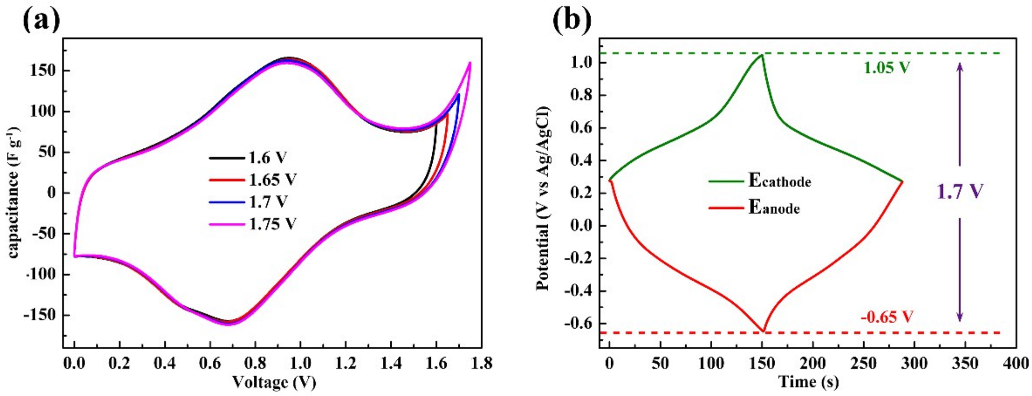

Figure S10 (a) CV curves under different voltage windows for asymmetric device. (b) In situ potential-time curves of cathode and anode at 1A g^{-1} at room temperature

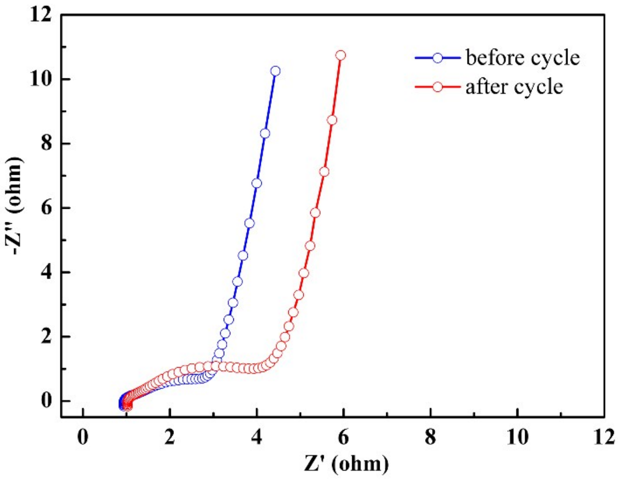

Figure S11 Nyquist plots for asymmetric device which is before and after the charge/discharge cycle at room temperature.

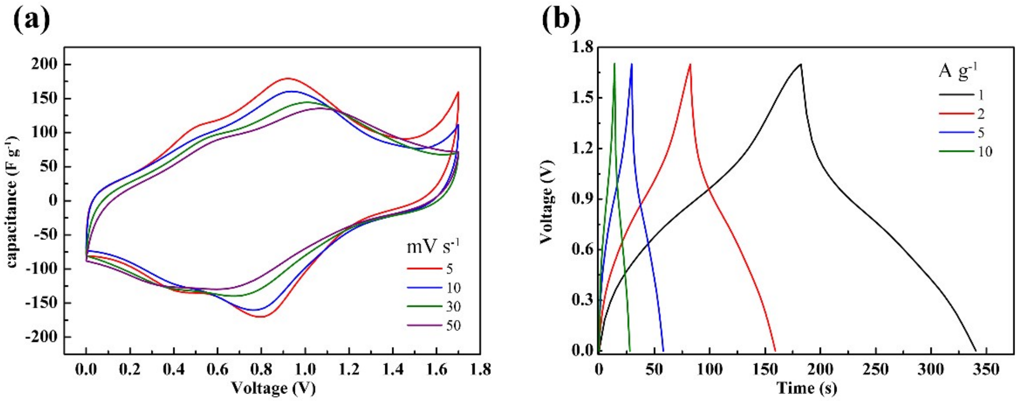

Figure S12 (a) CVs of the asymmetric device in gel electrolyte at different scan rate. (b) CDs of the asymmetric device in gel electrolyte at different current density at room temperature.

Table S1 Comparison of the electrochemical performance of supercapacitor recently reported at room temperature.

Materials	Electrolyte	Voltage window	Capacitance of cell (F g^{-1})	Current density	Energy density (Wh kg^{-1})	Power density (W kg^{-1})	Cycle numbers	Capacity retention	Ref
$Ti_3C_2T_x$//rGO	1 M H_2SO_4	1.1 V	48	2 mV s^{-1}	8	50	1000	76%	[1]
$Ti_3C_2T_x$ @NC//$Ti_3C_2T_x$ @NC	1 M H_2SO_4	1.1 V	176.9	1 A g^{-1}	29.7	582.3	5000	91.9%	[2]
G@MnO_2//porous graphene	1 M Na_2SO_4	2 V	56	0.5 A g^{-1}	30.6	197	10000	91.5%	[3]
$Ti_3C_2T_x$-Bi_2O_3//$Ti_3C_2T_x$-Bi_2O_3	1 M KOH	1.2 V	76	0.5 A g^{-1}	15.2	567	5000	85%	[4]
$Ti_3C_2T_x$//PEDOT@rGO	3 M H_2SO_4	1.4 V	47	5 mV s^{-1}	13	170	10000	80%	[5]
$Ti_3C_2T_x$//PPy@rGO	3 M H_2SO_4	1.4 V	59	5 mV s^{-1}	16	200	20000	75%	
$Ti_3C_2T_x$// PANI@rGO	3 M H_2SO_4	1.45 V	57	5 mV s^{-1}	17	200	20000	88.42%	
Ti_3C_2//TC-9	1 M KOH	1.5 V	49.3	1 A g^{-1}	15.4	750.2	5000	82.4%	[6]
$Ti_3C_2T_x$//RuO_2	1 M H_2SO_4	1.5 V	93	5 mV s^{-1}	29	3800	20000	86%	[7]
					24	26000			
PPy/rGO//NCs	3 M LiCl	1.6 V	43.2	20 mV s^{-1}	15.8	140	10000	88.7%	[8]
$MnCo_2S_4$//rGO	3 M KOH	1.6 V	88	1 A g^{-1}	31.3	800	5000	89%	[9]
400-KOH-Ti_3C_2//400-KOH-Ti_3C_2	1 M H_2SO_4	1.6 V	66.4	1 A g^{-1}	23.6	300	5000	90.4%	[10]
$Ti_3C_2T_x$//rGO	3 M H_2SO_4 +50 mM LiBr	1.8 V	76.5	1 A g^{-1}	34.4	1000	10000	—	[11]
					23.7	22500			
N-$Ti_3C_2T_x$ //HG2	1 M H_2SO_4	1.7 V	102	0.5 A g^{-1}	41	425	18000	83%	a
					26.7	42500			a

a This work

References

[1] A.M. Navarro-Suárez, K.L. Van Aken, T. Mathis, T. Makaryan, J. Yan, J. Carretero-González, T. Rojo, Y. Gogotsi, Development of asymmetric supercapacitors with titanium carbide-reduced graphene oxide couples as electrodes, Electrochimica Acta, 259 (2018) 752-761.

[2] T. Zhao, J. Zhang, Z. Du, Y. Liu, G. Zhou, J. Wang, Dopamine-derived N-doped carbon decorated titanium carbide composite for enhanced supercapacitive performance, Electrochimica Acta, 254 (2017) 308-319.

[3] L. Wang, Y. Ouyang, X. Jiao, X. Xia, W. Lei, Q. Hao, Polyaniline-assisted growth of MnO2 ultrathin nanosheets on graphene and porous graphene for asymmetric supercapacitor with enhanced energy density, Chemical Engineering Journal, 334 (2018) 1-9.

[4] Q.X. Xia, N.M. Shinde, J.M. Yun, T. Zhang, R.S. Mane, S. Mathur, K.H. Kim, Bismuth Oxychloride/MXene symmetric supercapacitor with high volumetric energy density, *Electrochimica Acta*, 271 (2018) 351-360.

[5] M. Boota, Y. Gogotsi, MXene-Conducting Polymer Asymmetric Pseudocapacitors, Advanced Energy Materials, 9 (2019) 1802917.

[6] Z. Pan, F. Cao, X. Hu, X. Ji, A facile method for synthesizing CuS decorated Ti_3C_2 MXene with enhanced performance for asymmetric supercapacitors, Journal of Materials Chemistry A, 7 (2019) 8984-8992.

[7] Q. Jiang, N. Kurra, M. Alhabeb, Y. Gogotsi, H.N. Alshareef, All Pseudocapacitive MXene-RuO_2 Asymmetric Supercapacitors, Advanced Energy Materials, 8 (2018) 1703043.

[8] J. Zhu, T. Feng, X. Du, J. Wang, J. Hu, L. Wei, High performance asymmetric supercapacitor based on polypyrrole/graphene composite and its derived nitrogen-doped carbon nano-sheets, Journal of Power Sources, 346 (2017) 120-127.

[9] S. Liu, S.C. Jun, Hierarchical manganese cobalt sulfide core–shell nanostructures for high-performance asymmetric supercapacitors, Journal of Power Sources, 342 (2017) 629-637.

[10] J. Li, X. Yuan, C. Lin, Y. Yang, L. Xu, X. Du, J. Xie, J. Lin, J. Sun, Achieving High Pseudocapacitance of 2D Titanium Carbide (MXene) by Cation Intercalation and Surface Modification, Advanced Energy Materials, 7 (2017) 1602725.

[11] S. Wang, X. Zhao, X. Yan, Z. Xiao, C. Liu, Y. Zhang, X. Yang, Regulating Fast Anionic Redox for High-Voltage Aqueous Hydrogen-Ion-based Energy Storage, Angewandte Chemie, 58 (2019) 205-210.